Molecular Cancer Therapeutics

AKT Inhibition Modulates H3K4 Demethylase Levels in PTEN-Null Prostate Cancer

Mohammad Imran Khan[1,2,3], Abid Hamid[3,4], Suvasmita Rath[3], Bushra Ateeq[5], Qateeb Khan[3], Imtiaz A. Siddiqui[3], Vaqar Mustafa Adhami[3], Hani Choudhry[1,2], Mazin A. Zamzami[1,2], and Hasan Mukhtar[3]

Abstract

Hyperactivated AKT kinase due to loss of its negative regulator PTEN influences many aspects of cancer biology, including chromatin. AKT primarily regulates acetyl-CoA production and phosphorylates many histone-modulating enzymes, resulting in their activation or inhibition. Therefore, understanding the therapeutic impact of AKT inhibition on chromatin-related events is essential. Here, we report that AKT inhibition in prostate-specific PTEN knockout mice significantly induces di- and trimethylation of H3K4 with concomitant reduction in H3K9 acetylation. Mechanistically, we observed that AKT inhibition reduces expression of the H3K4 methylation-specific histone demethylases KDM5 family, especially KDM5B expression at transcriptional levels. Furthermore, we observed that AKT negatively regulates miR-137 levels, which transcriptionally represses KDM5B expression. Overexpression of miR-137 significantly reduced KDM5B and increased H3K4 methylation levels but failed to change AKT phosphorylation. Overall, we observed that AKT transcriptionally regulates KDM5B mainly via repression of miR-137. Our data identify a mechanism by which AKT kinase modulates the prostate cancer epigenome through regulating H3K4 methylation. Additional studies on AKT inhibition–mediated induction of H3K4 methylation will help in designing strategies to enhance the therapeutic efficacy of PI3K/AKT inhibitors.

Introduction

Our knowledge regarding cancer initiation, propagation, and therapy resistance has received renewed attention as these events are highly governed and regulated by epigenetic machinery. The epigenetic machinery, that is, histone acetyltransferases, methyltransferases, and demethylases are regulated at both expression and activity levels by many factors that include growth and survival kinases. Among them, serine and threonine kinase AKT also known as protein kinase B (PKB) has evolved as a major kinase that regulates expression and activity of various chromatin modifiers.

Recently, AKT activation in tumorigenic conditions have been known to not only regulate oncogenic signaling but can also modulate the metabolism of tumorigenic cells. Activated AKT facilitates higher glucose uptake and increased acetyl-CoA production mainly by stimulating ATP-citrate-lyase (ACLY) enzymatic activity through phosphorylation at Ser^{455} site within the activation loop (1, 2). Indeed, hyperactivated Akt results in increased histone acetylation and phosphorylation of ACLY under both *in vitro* as well as *in vivo* conditions (3). The AKT-mediated hyperactivation of ACLY derives increased conversion of glucose-derived citrate into acetyl-CoA, which is a main donor of acetyl group required for protein acetylation (4). Therefore, Akt activation leads to sustained histone acetylation in several cancer types by altering acetyl-CoA concentrations. The impact of activated AKT is not only limited to histone acetylation, but also modulates histone methylation. AKT phosphorylates the major component of polycomb repressive complex 2 (PRC2) namely Enhancer of zeste homolog 2 (EZH2), an H3K27 histone methyltransferase, inhibiting its methyltransferase activity and reducing overall repressive histone mark H3K27me3 (5). The impact of AKT-mediated phosphorylation switches EZH2 from transcriptional repressor to a transcriptional coactivator of target oncogenic genes (6).

Furthermore, AKT facilitates the repression of tumor suppressor genes like CDKN2A by phosphorylating BMI, a polycomb repressive complex 1 (PRC1) involved in gene repression (7). Apart from methyltransferases, AKT phosphorylates histone acetyltransferase MOZ to regulate the expression of senescence-associated genes (8). All the above-mentioned reports clearly present a global impact of AKT on acetylation and methylation events related to histones. However, it remains unclear whether AKT regulates the function and expression of

[1]Department of Biochemistry, Faculty of Science, King Abdulaziz University, Jeddah, Saudi Arabia. [2]Cancer Metabolism and Epigenetic Unit, Faculty of Science, King Abdulaziz University, Jeddah, Saudi Arabia. [3]Department of Dermatology, School of Medicine and Public Health, University of Wisconsin, Madison, Wisconsin. [4]Cancer Pharmacology Division, CSIR-Indian Institute of Integrative Medicine, Canal Road, Jammu, India. [5]Molecular Oncology Lab, Department of Biological Sciences & Bioengineering, Indian Institute of Technology-Kanpur (IIT-K) Kanpur, India.

Note: Supplementary data for this article are available at Molecular Cancer Therapeutics Online (http://mct.aacrjournals.org/).

Corresponding Author: Mohammad Imran Khan, Department of Biochemistry, Faculty of Science, King Abdulaziz University, Jeddah 21589, Saudi Arabia. Phone: 608-263-3927; Fax: 608-263-5223; E-mail: mad4res@gmail.com

doi: 10.1158/1535-7163.MCT-18-0141

histone demethylases and, if so, whether this AKT-mediated regulation is critical for oncogenic growth.

Here, we report that AKT inhibition dramatically represses histone demethylases especially KDM5B expression at transcriptional level. Furthermore, we observed that AKT represses expression of KDM5B via targeting miR-137. Forced miR-137 expression reduces KDM5B and induces H3K4me3 levels under conditions of heightened AKT. Our work provides a novel mechanism for AKT-mediated regulation of prostate cancer epigenome.

Materials and Methods

Cell culture

All the cell lines (nontumorigenic and tumorigenic cell lines) used in this work were obtained from ATCC. The cell lines were characterized and authenticated by ATCC using a comprehensive database of short tandem repeat DNA profiles. All cell lines were well maintained in the laboratory based on the guidelines suggested by ATCC.

Generation of the prostate-specific Pten floxed: ProBasin-Cre4 (Pten-KO) mouse

We generated the mice in our laboratory by crossing Pten floxed (loxp/loxp) with PB-Cre (PB-Cre4Þ) as described earlier (9). The mice used were from the similar C57/BL6J background. The Jackson Laboratory mice (Pten floxed) were primarily screened for the floxed 328 bp band and/or wild-type 156 bp band by using the forward primer IMR9554: caagcactctgcgaactgag and reverse primer IMR9555: aagtttttgaaggcaagatgc. PB-Cre4 mice were obtained from the NCI Mouse Repository and were screened for the transgene (393 bp) using the mentioned primers; forward primer P021: ctgaagaatgggacaggcattg and reverse primer C031: catcactcgttgcatcgacc. The colonies of animals were maintained at the local animal resources facility of the University of Wisconsin-Madison (UW-Madison, WI). The University's Research Animal Resources Committee approved all of the animal protocols in accordance with the NIH Guidelines for the Care and Use of Laboratory Animals.

AKT inhibitor treatment to intact Pten-KO mice

Twenty intact Pten-KO mice were selected and used to determine the effect of perifosine (an AKT inhibitor; catalog number S1037 Selleckchem; ref. 10) on prostate tumor growth. The mice were equally divided into two groups (a) control (vehicle only; $n = 10$) and (b) AKT inhibitor (perifosine 30 mg/kg bodyweight; $n = 10$). Treatment of perifosine started at 7 weeks of age and continued until mice were sacrificed. Simultaneously, control groups of mice were treated with vehicle (PBS: DMSO) only. After the end of the dosing schedules, all mice from both groups were sacrificed at the end of 12 weeks and tissues were harvested and stored for analysis of various biochemical parameters and histone post-translational modifications (PTM).

Histone extraction

In vivo histone extraction was performed in both groups by using a commercially available kit from Epigentek Inc. (EpiQuik Total Histone Extraction Kit catalog number: OP-0006-100). Briefly, for histone isolation, 1 to 2 mg mouse tissues were used. Protein estimation of isolated histones was done using standard BSA method and isolated histones were stored at −80°C for storage and further use.

Knockdown/overexpression using small RNA interference

Human SMARTpool ON-TARGETplus AKT1 siRNA (L-003000-00-0005 5 nmol), Human SMARTpool ON-TARGETplus AKT2 siRNA (L-003001-00-0005 5 nmol), and nontargeting siRNA (D-001210-01-05) were purchased from Dharmacon and transfection was performed using well-established manufacturer's protocol.

Real-time qPCR analysis for mRNA expression

Briefly, RNA was extracted from the nontumorigenic, tumorigenic (PC3) and mouse tumor tissue (Pten-KO mice) samples using RNeasy Kit (Qiagen), and reverse transcribed with iScript Reverse Transcription SuperMix Kit (Bio-Rad). cDNA (1–100 ng) was amplified in triplicate using gene-specific primers;

mKdm5a Fw: GTTTCTTAAGGTGGCAAGTC Rv:TCTTTTGTAC-TGTTCCCTAC;
mKdm5b Fw: AGCTTTCTCAGAATGTTGGCRv:GCAGAGTCTG-GGAATTCACA;
mKdm5c Fw: GGGTTTCTAAAGTGTAGATCT Rv:CCACACA-TCTGAGCTTTAGT;
mKdm5d Fw: ATCTCCTCACCTCTCCAAAG Rv:TTGTCTCTA-GGCGTGGCCGT.

Threshold cycle (C_T) values obtained from the instrument's software were used to calculate the fold change of the respective mRNAs. ΔC_T was calculated by subtracting the C_T value of the housekeeping gene from that of the mRNA of interest. $\Delta\Delta C_T$ for each mRNA was then calculated by subtracting the C_T value of the control from the experimental value. Fold change was calculated by the formula $2^{-\Delta\Delta C_T}$.

Transfection with pre-miRs

The individual precursors of miRNAs (pre-miR) used in this study were purchased from Invitrogen. Cells were transfected with pre-miRs at 100 nmol/L working concentration, using Lipofectamine RNAiMAX (Invitrogen) according to the manufacturer's protocol (http://tools.thermofisher.com/content/sfs/manuals/Lipofectamine_RNAiMAX_Reag_protocol.pdf). Pre-miR negative control #1 (Invitrogen) was used as a scrambled control. Treatment proceeded for 72 hours before RNA extraction and/or Western blot analysis.

RNA purification and miRNA quantitative PCR

Extraction of miRNA was carried out by using a commercially available kit from Qiagen (miRNeasy Kit catalog number # 217004) following the manufacturer's instructions (https://www.qiagen.com/us/shop/sample-technologies/rna/total-rna/rneasy-mini-kit/#orderinginformation). For miRNA quantitative PCRs, total RNA (10 ng) was reverse transcribed with the TaqMan MicroRNA Reverse Transcription Kit (Applied Biosystems) and miRNA-specific primers. For miRNA quantitation, the 7500 Fast Real-Time System (Applied Biosystems) was used in conjunction with gene-specific TaqMan assay kits for miR-137, miR-138, and RNU6B. RNU6B was used as an endogenous control to normalize the expression of target miRNAs.

Analysis of histone PTMs

ELISA-Based Quantification Kit was used to measure global histone H3 modifications. Briefly, H3 modification multiplex array (EpiQuik Histone H3 Modification Multiplex Assay Kit,

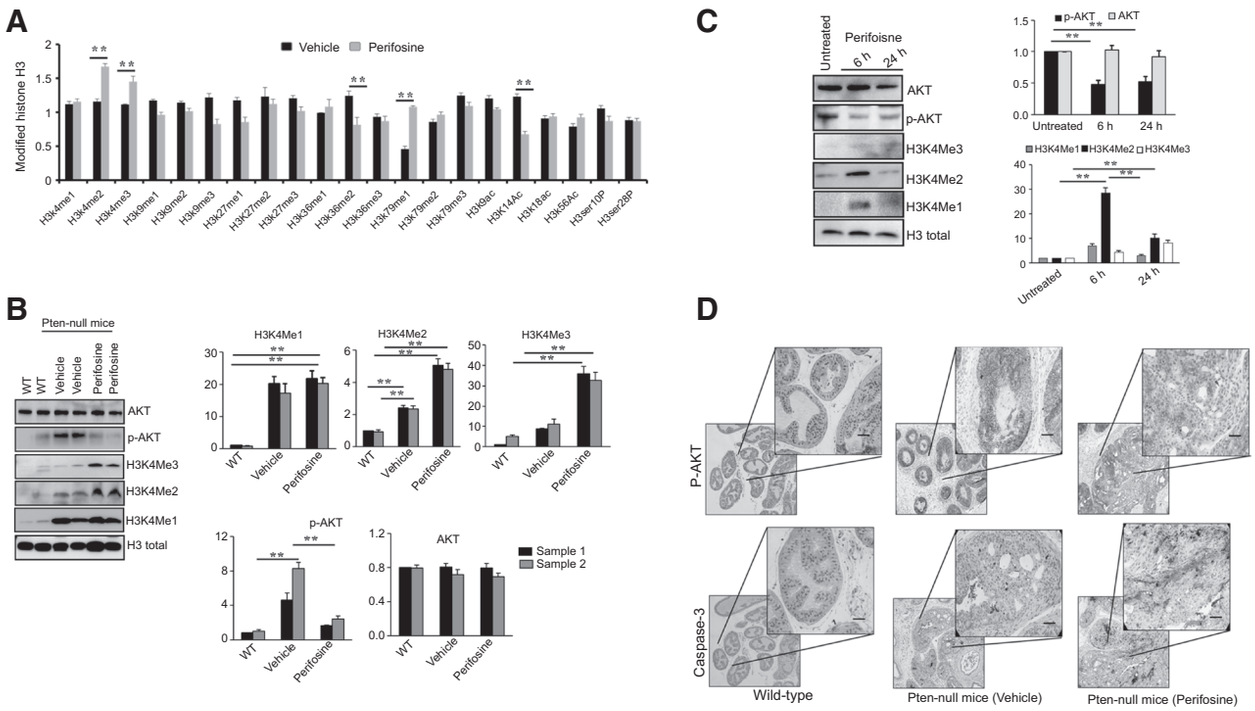

Figure 1.

AKT kinase inhibition modulates global epigenome marks and induces H3K4 methylation. **A,** Histograms show fold change in H3 histone modifications after treatment with AKT inhibitor perifosine using the Epiquick Histone Modification Multiplex Assay Kit in PTEN-deficient *in vivo* samples. Error bars, SEM. **B,** Western blot analysis ($n = 3$) of tissue extracts isolated from wild-type and PTEN-knockout mice samples after perifosine treatment showing expression pattern of H3K4Me1/2/3 proteins. **C,** Western blot analysis ($n = 3$) of perifosine-treated PTEN-null PC3 cell lines at 6- and 24-hour time point. Total H3 histone was used as loading control. **D,** Representative photomicrographs (magnification, ×10 and ×40) showing IHC staining for p-AKT and caspase-3 in Pten wild-type and knockout tumor sections of vehicle- or perifosine-treated mice.

#P-3100-96, Epigentek) was used. Equal amounts of protein samples were added in each independent experiment; however, overall protein concentration range was from 100 to 300 ng. H3 modifications were calculated according to the manufacturer's instructions, which also accounts for protein amounts, and the final values for each modification were presented as the percentage over untreated control.

H3K4 demethylase activity assay

The H3K4-specific demethylase activity was performed by using a commercially available kit from Abcam [KDM5/JARID Activity Quantification Assay Kit (Colorimetric) # ab113463]. The JARID Demethylase Assay Kit was capable of measuring activity or inhibition of total JARID subtypes and required cellular nuclear extracts.

IHC analysis

Sections (4–8 μm) were obtained from the fixed blocks of both tissue types (normal and tumor). Initially before starting the staining procedure, slides were warmed at room temperature for 5 minutes. Tissues were stained using anti-caspase 3 (Cell Signaling Technology; mab #9664) followed by goat anti-rabbit HRP-Polymer (Biocare) as a secondary antibody. Anti-pAkt^{ser473} (Cell Signaling Technology; mab #4060) was applied and goat anti-rabbit HRP-Polymer (Biocare) was used as a secondary antibody. DAB chromogen was used for both antibodies for detection. Data acquisition and image analysis were performed as per standard methodology.

In vivo tumor xenograft mouse study

Athymic (*nu/nu*) male nude mice (Harlan) were housed under pathogen-free conditions with a 12-hour light/dark schedule and fed with an autoclaved diet *ad libitum*. We chose PTEN-null PC3 cells for determining the *in vivo* effects of perifosine, DZNeP alone, and their combination. Thirty-two animals were then randomly divided into four groups, with 8 animals in each group. The first group of animals received intraperitoneal injection of vehicle (DMSO; 30 μL) and served as control. Furthermore, group 2 received intraperitoneal injection of perifosine (30 mg/kg bodyweight) twice weekly, group 3 received intraperitoneal injection of DZNeP (1 mg/kg bodyweight) twice weekly, and group 4 received intraperitoneal and intradermal injection of perifosine and DZNeP twice weekly. In both groups, the sizes of tumors were measured twice weekly (11). Once, the tumor size reaches to a volume of 1,200 mm^3 in the control group, all animals of both groups were sacrificed.

Statistical analysis

Data were analyzed using GraphPad Prism (version 5; GraphPad Software). Two-tailed, unpaired *t* test was used. Data points in graphs represent mean ± SD, and *P* values <0.05 were considered statistically significant.

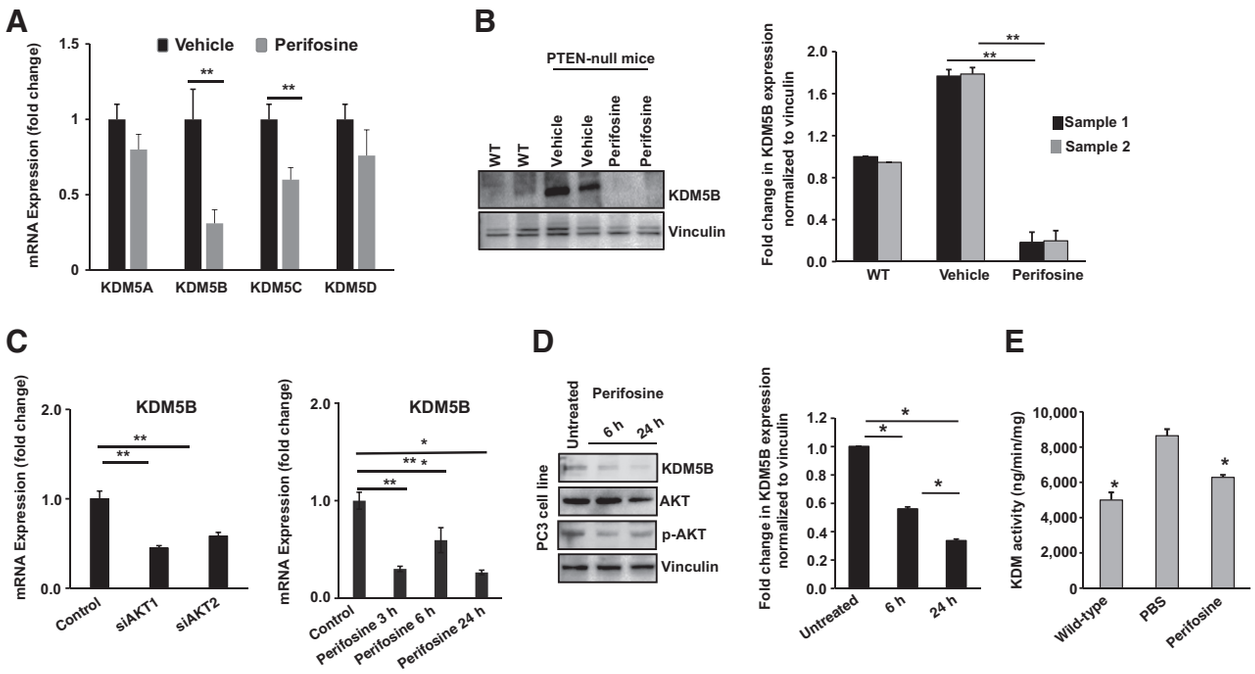

Figure 2.

AKT kinase inhibition reduces histone demethylase KDM5B. **A,** qPCR analysis of selective HDMs in AKT inhibitor–treated *in vivo* samples showing mRNA expression patterns. 18S actin was used as loading control. **B,** Western blot analysis ($n = 3$) of tissue extracts isolated from wild-type and PTEN-knockout mice samples in control as well as perifosine-treated conditions in duplicate. Vinculin was used as a loading control. Bars represent normalized data (mean ± SEM, $n = 3$); *, $P < 0.05$ **C,** PC3 cells transfected with nontarget siRNA and siRNA targeting AKT1 as well as AKT2. In another set of experiments, PC3 cells were treated with perifosine for 3, 6, and 24 hours. qPCR analysis of both experimental setups showed expression pattern of KDM5B mRNA. 18S actin was used as a loading control. **D,** Western blot analysis of whole-cell lysates isolated from PC3 cell after treatment with perifosine for 6 and 24 hours. Vinculin was used as a loading control. Histograms represent quantification of Western blot results normalized to loading control (mean ± SEM, $n = 3$); *, $P < 0.05$ **E,** *In vivo* histone demethylase (KDM5) activity assay of the nuclear lysates after perifosine treatment.

Results

In vivo AKT inhibition induces H3K4 methylation

To understand the global impact of *in vivo* AKT inhibition on histone (H3) modifications, histone protein samples were collected from vehicle and perifosine-treated Pten-KO mice. We observed a statistically significant upregulation of H3K4 di- and trimethylation in perifosine-treated samples when compared with control. We also noted a significant reduction in H3K9me3 and H3K36me2 along with statistically significant induction in H3K79me1. Furthermore, we found a statistically significant reduction in H3K14ac in perifosine-treated Pten-KO mice when compared with control (Fig. 1A). Our data suggest that AKT inhibition globally affects chromatin by modulating various histone marks. Because we observed a consistent reduction in H3K4 methylation levels, which was recently shown to be regulated by AKT kinase in breast cancer, we decided to focus on this histone mark in all further current studies.

We next evaluated by Western blotting the H3K4 methylation status in samples from *in vivo* as well as *in vitro* models treated with perifosine. We observed a statistically significant increase in expression of H3K4Me3 and H3K4Me2 levels in perifosine-treated Pten-KO mice samples when compared with vehicle (Fig. 1B), whereas no change was observed in H3K4Me1 level. Perifosine significantly suppressed AKT phosphorylation and dramatically effected the morphology of prostate in treated group (Fig. 1B; Supplementary Fig. S1A–S1C). Furthermore, H3K4 methylation status was validated in PTEN-null prostate cancer cell line PC3. In agreement with our *in vivo* results, we observed a statistically significant increase in H3K4me1/2/3 levels after 6 hours that showed a decrease at 24 hours when compared with untreated controls (Fig. 1C). We also observed a clear reduction in phospho-AKT levels at both time points. In addition, we also observed a clear reduction in phospho-AKT levels along with increase in staining intensity of caspase-3 (apoptosis marker) in perifosine-treated group when compared with vehicle-treated (Fig. 1D). Overall, we observed broad changes in various histone marks during inhibition of AKT kinase both *in vitro* and *in vivo*.

AKT inhibition reduces KDM5B expression level

The H3K4 di- and trimethylation is demethylated by the JARID1 subfamily of JmjC proteins, which encompasses four members: KDM5A (JARID1A), KDM5B (JARID1B), KDM5C (JARID1C), and KDM5D (JARID1D; refs. 12, 13). Because we observed H3K4 methylation mark changes during AKT kinase inhibition in our study and the KDM5 family of proteins is known to interfere in the AKT pathway (14), we decided to focus on this family of demethylases only.

First, we assessed the mRNA expression of all KDM5 family demethylases (KDM5A-D) in perifosine-treated Pten-KO mice

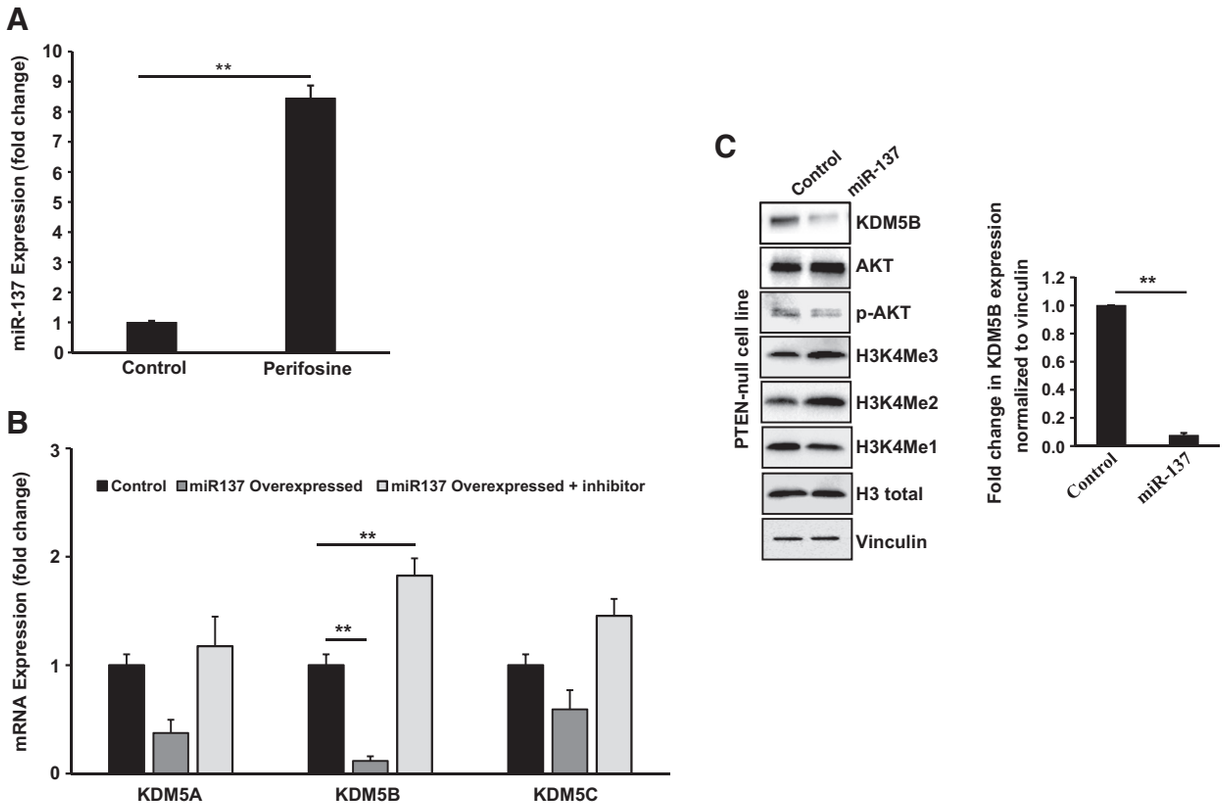

Figure 3.

AKT negatively regulates miR-137 expression to transcriptionally regulate KDM5B levels. **A,** Histograms represent pattern of miR-137 expression in samples isolated from perifosine-treated mice against control samples showed by qPCR. 18S actin was used as loading control. **B,** Histograms showing RNA levels of KDM family from PC3 cells transfected with miR-137 overexpression constructs and miR-137 inhibitor by qPCR. **C,** PC3 cells were transfected with miR-137–overexpressing constructs, and whole-cell lysates were analyzed by Western blotting to study the status of KDM5B protein along with p-AKT and H3K4 methylation marks. Vinculin was used as loading control. Bars depicting normalized data (mean ± SEM, $n = 3$); *, $P < 0.05$.

samples and observed a statistically significant reduction in KDM5B mRNA expression when compared with control (Fig. 2A). These observations led us to conclude that KDM5B is the AKT-targeted histone demethylase in our experiments. Second, we observed similar KDM5B protein expression using Western blot analysis ($n = 3$) in perifosine-treated Pten-KO mice samples when compared with control (Fig. 2B). We anticipated a mechanism that regulates KDM5B expression at transcriptional level after AKT inhibition. To assess this, KDM5B mRNA levels were estimated both in AKT1/2 siRNA as well as inhibitor-treated PTEN-null PC3 cells. In the first set of experiments, AKT1/2 siRNA were transfected to PC3 cells, whereas in the other experimental setup, PC3 cells were treated with AKT inhibitor perifosine for various time points, that is, 3, 6, and 24 hours. Our data showed a statistically significant decrease in KDM5B mRNA expression in both the experimental conditions after AKT inhibition (Fig. 2C). We also observed reduced KDM5B protein expression in samples isolated from PTEN-null PC3 cell lines after perifosine treatment for 6 and 24 hours (Fig. 2D). Finally, we measured KDM5 enzymatic activity in nuclear lysates and observed a significant reduction in KDM5 enzymatic activity in perifosine-treated Pten-KO mice samples when compared with control (Fig. 2E).

AKT inhibition induces miR-137 expression to transcriptionally regulate KDM5B levels

Various miRNAs are involved in AKT-regulatory network and are affected by alteration in AKT activity (15). To understand the transcriptional regulation of KDM5B by AKT, we focused on miR-137, as this has been shown to transcriptionally regulate H3K4 demethylases. Also, the involvement of miR-137 in the AKT pathway has been reported previously (16), and overexpression of miR-137 was shown to suppress PI3K/AKT activity in different model systems (17–19).

We found a statistically significant upregulation in miR-137 expression levels in perifosine-treated Pten-KO mice samples when compared with control. These findings were further confirmed in Pten-null PC3 cells treated with perifosine (Fig. 3A). Next, we investigated the effect of miR-137 overexpression on KDM5B expression at both transcriptional and translational levels. In the first experiment, PC3 cells were transfected with miR-137 construct alone or in combination with miR-137 inhibitor. Our results showed significant downregulation of KDM5B mRNA expression as compared with KDM5A and KDM5C, which was reverted after treatment with miR-137 inhibitor (Fig. 3B). Furthermore, we found that miR-137 overexpression significantly reduces KDM5B protein expression and concomitantly increases H3K4me3 and

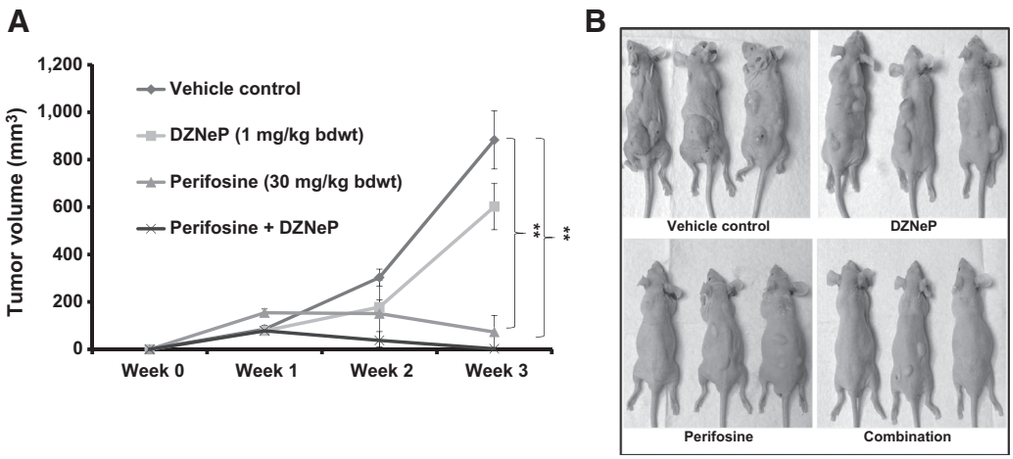

Figure 4.

Combination of AKT inhibitor with broad methyltransferase inhibitor synergize to reduce PTEN-null prostate cancer tumorigenicity. Effect of combination of AKT inhibitor (perifosine) and DZNeP (broad histone methylation inhibitor) on PTEN-null PC3 tumor growth in athymic nude mice. Approximately 1×10^6 PC3 cells were subcutaneously injected in each flank of the mouse to initiate tumor growth. Once tumors started to grow, their sizes were measured twice weekly and the tumor volume was calculated. **A,** Average tumor volume of vehicle, perifosine, DZNeP, and combination-treated mice plotted over weeks after tumor cell inoculation. Values represent mean ± SE of 6 animals. **, $P < 0.001$ versus the vehicle-treated group of mice. Details are described in Materials and Methods. **B,** Representative photographs of tumors bearing mice from each group.

H3K4me2 levels, confirming our earlier results. However, no change in phosphorylation status of AKT was observed (Fig. 3C). These results suggested that AKT transcriptionally regulates KDM5B levels mainly via repression of miR-137.

AKT inhibitor synergies with DZNeP

Because we observed a clear modification in various histone methylation marks during AKT kinase inhibition, we hypothesized that the combination of AKT inhibitor with a methyltransferase inhibitor such as DZNeP (20, 21) could provide better remission of PTEN-null–driven tumorigenicity and tumor growth. For this purpose, we implanted PTEN-null PC3 cell lines in NOD/SCID mice and treated them with either an AKT inhibitor alone or in combination with DZNeP. We then measured tumor volume for 3 weeks postimplantation. As hypothesized, we found a significant reduction in tumor volume in the combination-treated group when compared with groups treated alone with either AKT inhibitor or DZNeP alone (Fig. 4A and B).

Discussion

The major findings of the current work are as follows: (i) AKT inhibition induces global H3K4 methylation levels. (ii) AKT negatively regulates miR-137 to transcriptionally repress KDM5B expression. (iii) Forced expression of miR-137 reduces KDM5B and induces H3K4me3 levels. (iv) AKT inhibitor synergies with DZNeP to reduce tumorigenicity of PTEN-null prostate cancer cells. Inhibition of PI3K/AKT pathway plays a significant role in many prostate cancer therapeutics (22). A recent finding found that AKT inhibition reduces levels of H3K4 trimethylation levels in breast cancer cells (14). However, surprisingly we observed induction of H3K4me2/3 methylation levels in AKT inhibitor–treated PTEN-null prostate cancer models. We speculate that this discrepancy could be due to the use of a different model in our study. However, at the same time, it would be interesting to understand the impact of AKT inhibition on cellular localization of KDM5B and H3K4me2/3 along with their chromatin localization in our model. Our observations suggest that AKT-driven KDM5B expression is important for tumorigenicity of PTEN prostate cancer cells. This notion is supported by previous studies that also showed the protumorigenic role of KDM5B in prostate cancer (23–25).

We further conducted in-depth experiments to understand the transcriptional regulation of KDM5B by AKT kinase in PTEN-null prostate cancer. Aberrant KDM5B expression influences miRNA expression and affects cancer progression (26). Conversely, miRNA can also regulate KDM5B expression. A very recent finding explained KDM5B, as a target of miR-137 in breast cancer cells (27) that also reduced proliferative nature of breast cancer cells. Hence, we wanted to study the involvement of miRNAs in AKT-driven transcriptional regulation of KDM5B. Our results revealed a significant change in miR-137 mRNA expression in AKT inhibitor–treated PTEN-null samples. We further validated the effect of miR-137 overexpression and confirmed downregulation of KDM5B mRNA that is reverted after treatment with miR-137 inhibitor. Furthermore, increased KDM5B protein expression and induction of H3K4me2/3 methylation was also observed in miR-137–overexpressing PTEN-null cell lines. However, no change in AKT phosphorylation after miR-137 overexpression was observed. Therefore, we believe that miR-137 acts downstream of AKT kinase. However, this notion requires further validation. Our data regarding regulation of KDM5B expression by miR-137 in PTEN null conditions is in clear agreement with earlier studies (28, 29). The oncogenic roles of KDM5B are now well explored in prostate cancer; however, information regarding its regulation at both transcriptional and translational levels still remains scarce. Recently, Lu and colleagues 2015 (30) showed SKP2-mediated translational regulation of KDM5B protein expression in Pten/Trp53–mutant prostate cancer. Our novel observations now add an additional layer of KDM5B regulation at transcriptional levels in PTEN-null prostate cancer.

In conclusion, our data clearly identified a mechanism by which AKT alters the epigenome of prostate cancer, primarily through regulating H3K4 methylation and KDM5B expression. These data can be used in the future development of combination therapies using PI3K/AKT inhibitors and chromatin-modifying compounds in the treatment of PTEN-null prostate cancer. Our preclinical results clearly demonstrate the enhanced efficacy of AKT inhibitor in combination with histone methyltransferase inhibitor. These observations point toward the need of additional studies to devise novel strategies to enhance the therapeutic efficacy of PI3K/AKT inhibitors in PTEN-null prostate cancer that is currently in clinical development.

Disclosure of Potential Conflicts of Interest

No potential conflicts of interest were disclosed.

Authors' Contributions

Conception and design: M.I. Khan, A. Hamid, S. Rath, I.A. Siddiqui, V.M. Adhami, M.A. Zamzami, H. Mukhtar
Development of methodology: A. Hamid, S. Rath, B. Ateeq, Q. Khan, I.A. Siddiqui, H. Choudhry, H. Mukhtar
Acquisition of data (provided animals, acquired and managed patients, provided facilities, etc.): A. Hamid, I.A. Siddiqui, H. Mukhtar
Analysis and interpretation of data (e.-g., statistical analysis, biostatistics, computational analysis): M.I. Khan, A. Hamid, S. Rath, B. Ateeq, Q. Khan, I.A. Siddiqui, V.M. Adhami, H. Choudhry, H. Mukhtar
Writing, review, and/or revision of the manuscript: M.I. Khan, A. Hamid, S. Rath, I.A. Siddiqui, V.M. Adhami, H. Choudhry, H. Mukhtar
Administrative, technical, or material support (i.e., reporting or organizing data, constructing databases): M.I. Khan, A. Hamid, M.A. Zamzami, H. Mukhtar
Study supervision: M.I. Khan, V.M. Adhami, H. Mukhtar

Acknowledgments

We would like to thank Prof. John M. Denu and Ahmed Aljohani for their suggestions during manuscript proofreading. This work was supported by the United States Public Health Service grant RO1CA160867 (to H. Mukhtar).

The costs of publication of this article were defrayed in part by the payment of page charges. This article must therefore be hereby marked *advertisement* in accordance with 18 U.S.C. Section 1734 solely to indicate this fact.

Received February 5, 2018; revised September 24, 2018; accepted November 12, 2018; published first November 16, 2018.

References

1. Potapova IA, El-Maghrabi MR, Doronin SV, Benjamin WB. Phosphorylation of recombinant human ATP:citrate lyase by cAMP-dependent protein kinase abolishes homotropic allosteric regulation of the enzyme by citrate and increases the enzyme activity. Allosteric activation of ATP: citrate lyase by phosphorylated sugars. Biochemistry 2000;39:1169–79.
2. Berwick DC, Hers I, Heesom KJ, Moule SK, Tavare JM. The identification of ATP-citrate lyase as a protein kinase B (Akt) substrate in primary adipocytes. J Biol Chem 2002;277:33895–900.
3. Wellen KE, Hatzivassiliou G, Sachdeva UM, Bui TV, Cross JR, Thompson CB. ATP-citrate lyase links cellular metabolism to histone acetylation. Science 2009;324:1076–80.
4. Evertts AG, Zee BM, Dimaggio PA, Gonzales-Cope M, Coller HA, Garcia BA. Quantitative dynamics of the link between cellular metabolism and histone acetylation. J Biol Chem 2013;288:12142–51.
5. Cha TL, Zhou BP, Xia W, Wu Y, Yang CC, Chen CT, et al. Akt-mediated phosphorylation of EZH2 suppresses methylation of lysine 27 in histone H3. Science 2005;310:306–10.
6. Xu K, Wu ZJ, Groner AC, He HH, Cai C, Lis RT, et al. EZH2 oncogenic activity in castration-resistant prostate cancer cells is Polycomb-independent. Science 2012;338:1465–9.
7. Liu Y, Liu F, Yu H, Zhao X, Sashida G, Deblasio A, et al. Akt phosphorylates the transcriptional repressor bmi1 to block its effects on the tumor-suppressing ink4a-arf locus. Sci Signal 2012;5:ra77.
8. Rokudai S, Laptenko O, Arnal SM, Taya Y, Kitabayashi I, Prives C. MOZ increases p53 acetylation and premature senescence through its complex formation with PML. Proc Natl Acad Sci U S A 2013;110:3895–900.
9. Wang S, Gao J, Lei Q, Rozengurt N, Pritchard C, Jiao J, et al. Prostate-specific deletion of the murine Pten tumor suppressor gene leads to metastatic prostate cancer. Cancer Cell 2003;4:209–21.
10. Patel V, Lahusen T, Sy T, Sausville EA, Gutkind JS, Senderowicz AM. Perifosine, a novel alkylphospholipid, induces p21(WAF1) expression in squamous carcinoma cells through a p53-independent pathway, leading to loss in cyclin-dependent kinase activity and cell cycle arrest. Cancer Res 2002;62:1401–9.
11. Khan N, Bharali DJ, Adhami VM, Siddiqui IA, Cui H, Shabana SM, et al. Oral administration of naturally occurring chitosan-based nanoformulated green tea polyphenol EGCG effectively inhibits prostate cancer cell growth in a xenograft model. Carcinogenesis 2014;35:415–23.
12. Cloos PA, Christensen J, Agger K, Helin K. Erasing the methyl mark: histone demethylases at the center of cellular differentiation and disease. Genes Dev 2008;22:1115–40.
13. Mosammaparast N, Shi Y. Reversal of histone methylation: biochemical and molecular mechanisms of histone demethylases. Annu Rev Biochem 2010;79:155–79.
14. Spangle JM, Dreijerink KM, Groner AC, Cheng H, Ohlson CE, Reyes J, et al. PI3K/AKT signaling regulates H3K4 methylation in breast cancer. Cell Rep 2016;15:2692–704.
15. Xu M, Mo YY. The Akt-associated microRNAs. Cell Mol Life Sci 2012;69: 3601–12.
16. Liang L, Li X, Zhang X, Lv Z, He G, Zhao W, et al. MicroRNA-137, an HMGA1 target, suppresses colorectal cancer cell invasion and metastasis in mice by directly targeting FMNL2. Gastroenterology 2013;144: 624–35.
17. Zhang B, Ma L, Wei J, Hu J, Zhao Z, Wang Y, et al. miR-137 suppresses the phosphorylation of AKT and improves the dexamethasone sensitivity in multiple myeloma cells via targeting MITF. Curr Cancer Drug Targets 2016;16:807–17.
18. Thomas KT, Anderson BR, Shah N, Zimmer SE, Hawkins D, Valdez AN, et al. Inhibition of the schizophrenia-associated microRNA miR-137 disrupts Nrg1alpha neurodevelopmental signal transduction. Cell Rep 2017; 20:1–12.
19. Qin Y, Zhang S, Deng S, An G, Qin X, Li F, et al. Epigenetic silencing of miR-137 induces drug resistance and chromosomal instability by targeting AURKA in multiple myeloma. Leukemia 2017;31:1123–35.
20. Miranda TB, Cortez CC, Yoo CB, Liang G, Abe M, Kelly TK, et al. DZNep is a global histone methylation inhibitor that reactivates developmental genes not silenced by DNA methylation. Mol Cancer Ther 2009; 8:1579–88.
21. Zeybel M, Luli S, Sabater L, Hardy T, Oakley F, Leslie J, et al. A proof-of-concept for epigenetic therapy of tissue fibrosis: inhibition of liver fibrosis progression by 3-deazaneplanocin A. Mol Ther 2017;25:218–31.
22. Morgan TM, Koreckij TD, Corey E. Targeted therapy for advanced prostate cancer: inhibition of the PI3K/Akt/mTOR pathway. Curr Cancer Drug Targets 2009;9:237–49.
23. Xiang Y, Zhu Z, Han G, Ye X, Xu B, Peng Z, et al. JARID1B is a histone H3 lysine 4 demethylase up-regulated in prostate cancer. Proc Natl Acad Sci U S A 2007;104:19226–31.
24. Lee HY, Yang EG, Park H. Hypoxia enhances the expression of prostate-specific antigen by modifying the quantity and catalytic activity of Jumonji C domain-containing histone demethylases. Carcinogenesis 2013;34: 2706–15.

25. Han M, Xu W, Cheng P, Jin H, Wang X. Histone demethylase lysine demethylase 5B in development and cancer. Oncotarget 2017;8:8980–91.
26. Bamodu OA, Huang WC, Lee WH, Wu A, Wang LS, Hsiao M, et al. Aberrant KDM5B expression promotes aggressive breast cancer through MALAT1 overexpression and downregulation of hsa-miR-448. BMC Cancer 2016; 16:160.
27. Denis H, Van Grembergen O, Delatte B, Dedeurwaerder S, Putmans P, Calonne E, et al. MicroRNAs regulate KDM5 histone demethylases in breast cancer cells. Mol Biosyst 2016;12:404–13.
28. Nilsson EM, Laursen KB, Whitchurch J, McWilliam A, Odum N, Persson JL, et al. MiR137 is an androgen regulated repressor of an extended network of transcriptional coregulators. Oncotarget 2015;6:35710–25.
29. Daniunaite K, Dubikaityte M, Gibas P, Bakavicius A, Rimantas Lazutka J, Ulys A, et al. Clinical significance of miRNA host gene promoter methylation in prostate cancer. Hum Mol Genet 2017;26:2451–61.
30. Lu W, Liu S, Li B, Xie Y, Adhiambo C, Yang Q, et al. SKP2 inactivation suppresses prostate tumorigenesis by mediating JARID1B ubiquitination. Oncotarget 2015;6:771–88.